

LETTER TO THE EDITOR

Lifetime measurements in Tl II

M Henderson and L J Curtis

Department of Physics and Astronomy, University of Toledo, Toledo, OH 43606, USA

Received 10 June 1996

**Abstract.** Lifetimes are reported for the  $6s6p\ ^1\text{P}_1$ ,  $6s6d\ ^1\text{D}_2$  and  $6s7s\ ^1\text{S}_0$  levels in Hg-like Tl II, measured using beam-foil excitation. The values obtained were  $\tau(^1\text{P}_1) = 0.59 \pm 0.02$  ns,  $\tau(^3\text{P}_1) = 39 \pm 2$  ns,  $\tau(^1\text{D}_2) = 6.5 \pm 0.5$  ns, and  $\tau(^1\text{S}_0) = 3.0 \pm 0.4$  ns. Isoelectronic trends for line strengths of the resonance and intercombination transitions are studied through comparisons with earlier measurements for Hg I–Bi IV.

We report here lifetime measurements of the  $6s6p\ ^1\text{P}_1$ ,  $6s6p\ ^3\text{P}_1$ ,  $6s6d\ ^1\text{D}_2$ , and  $6s7s\ ^1\text{S}_0$  levels in singly ionized thallium in the mercury isoelectronic sequence. This sequence is the heaviest homologue in the group II-B alkaline-earth Zn-, Cd- and Hg-like systems, which have  $(n-1)d^{10}ns^2$  ground configurations. Oscillator strength data for Tl II are needed for many specific applications. Spectral lines from Tl II have been identified in astrophysical observations of Hg–Mn-type stars made using the Goddard high resolution spectrograph on board the Hubble space telescope [1, 2]. Because it can be confined in an ion trap and possesses a very long-lived metastable  $6s6p\ ^3\text{P}_0$  level, Tl II can be utilized as a high accuracy atomic clock [3]. In terms of fundamental theory, the 80-electron Hg isoelectronic sequence provides a severe challenge to existing calculational methods [4, 5], which can only be tested by acquiring a base of reliable measurements. Moreover, semi-empirical regularities have been observed [6] which may permit the interpolation of line strengths of the resonance and intercombination lines to be made based on a few precise measurements at low stages of ionization and an asymptotic high- $Z$  limit [7, 8]. Earlier curve fitting studies have been made [9–11] for the  $^1\text{P}_1$ ,  $^1\text{D}_2$  and  $^1\text{S}_0$  levels, but this is the first lifetime measurement of the  $^3\text{P}_1$  level, and the first cascaded–correlated [12, 13] lifetime measurement of the  $^1\text{P}_1$  level.

The measurements utilized the 300 kV University of Toledo heavy ion accelerator. Detailed descriptions of this facility can be found in reports of earlier studies in this series (e.g. [14, 15]) as well as in instrumentation reviews [16, 17]. Ions of  $\text{Tl}^{2+}$  were produced in the ion source, accelerated through 20 kV, and magnetically analysed. After momentum and mass-to-charge selection, the ions were post-accelerated to final energies of 500 keV for study of the resonance line, and 520 keV for study of the intercombination line. The ions then entered an electrostatic switchyard and were steered into the experimental station and collimated before passage through a thin carbon foil (ranging from  $2.1\text{--}2.5\ \mu\text{g cm}^{-1}$ ). At beam energies of 500–520 keV, the observed spectroscopic excitations were primarily in Tl II, Tl III, and Tl IV.

The Tl II emission lines were analysed with an Acton 1-m normal incidence VUV monochromator, with three sets of concave gratings and detectors: a 1200 lines/mm grating coupled with a solar blind detector for the region  $\lambda 1321.7\ \text{\AA}$  transition; a 1200 lines/mm

grating coupled with a bialkali detector for the  $\lambda 1908.7 \text{ \AA}$  transition; and a 600 lines/mm grating coupled with a bialkali detector for the  $\lambda 2531$  and  $3092 \text{ \AA}$  transitions. The post-foil velocity was determined to within 2.5% by taking into account uncertainties in energy calibration, foil thickness, and possible beam divergence.

Using the Danfysik model 911A ion source, ions were obtained from pure thallium metal. To minimize foil breakage, the current was limited to less than 200 nA (100 particle nA for  $\text{Tl}^{2+}$ ). It was relatively easy to produce  $\text{Tl}^{2+}$  currents greater than 200 nA, and it was possible to obtain currents approaching  $1 \mu\text{A}$ . The methods used to obtain doubly charged thallium in the ion source are similar to those used earlier for obtaining  $\text{Cd}^{2+}$ , and are discussed in [15].

Due to the nonselective nature of beam-foil excitation, the level populations (and hence the decay curves) are affected by cascade repopulation. Thus, while they produce a negligible contribution in the case of long-lived decays such as the  $6s^2 \text{ } ^1\text{S}_0$ – $6s6p \text{ } ^3\text{P}_1$  intercombination transition, cascades can distort the decay curves of shorter-lived levels such as the  $6s^2 \text{ } ^1\text{S}_0$ – $6s6p \text{ } ^1\text{P}_1$  resonance transition, which is repopulated by the yrast chain through the  $6s6p \text{ } ^1\text{P}_1$ – $6s6d \text{ } ^1\text{D}_2$  transitions, as well as by Rydberg transitions such as  $6s6p \text{ } ^1\text{P}_1$ – $6s7s \text{ } ^1\text{S}_0$ . Situations in which cascading is dominated by a few strong channels are ideally suited to analysis by the ANDC method [12, 13], which performs a joint analysis of the decay curves of the level of interest together with those of levels that directly repopulate it.

The decay curves were all analysed by the multiexponential fitting program DISCRETE [18]. In the case of the  $6s6p \text{ } ^1\text{P}_1$  resonance transition this was supplemented by ANDC analyses made jointly with the  $6s6d \text{ } ^1\text{D}_2$  and  $6s7s \text{ } ^1\text{S}_0$  decay curves. Two ANDC codes were used: one makes use of the numerical differentiation of the raw data; the other utilized the program CANDY [19], which uses data that have been smoothed through the application of a multiexponential filter. The uncertainties in our multiexponential fits were computed by combining statistical uncertainties in the individual fits, scatter among the independent measurements and estimates of possible errors introduced by cascade corrections.

For the DISCRETE fits of each of the three singlet decay curves the primary exponential was much stronger than, and well separated in effective lifetime from, the cascade contributions. Thus, while ANDC analysis reduced the uncertainties in the determination of the lifetime of the resonance transition, it did not significantly alter the extracted value. The intercombination transition was well represented by a single exponential, and estimates [20] of possible beam divergence caused by multiple scattering in the foil indicated that more than 95% of the beam particles were within the volume viewed by the optical system over the full range of the decay curves. The results of our lifetime measurements are given in table 1, and compared with earlier measurements and theoretical calculations. Comparisons of the degree of core–valence and core–core correlation included in these calculations are given in [4]. Our lifetime measurements for the resonance and intercombination transitions correspond to absorption oscillator strength values  $f(\text{Res}) = 1.33(9)$  and  $f(\text{Int}) = 0.042(2)$ .

We have also examined the isoelectronic trends of the lifetimes of the resonance and intercombination levels using an energy-level-based reduction of the line strengths. For  $ns^2 \text{ } ^1\text{S}_0$ – $nsnp \text{ } ^{1,3}\text{P}_1$  transitions  $LS$  notation is valid for the lower level but is only nominal for the upper level, since it is spin-hybridized by intermediate coupling. In the absence of configuration interaction, the spin hybridization of the  $nsnp$  configuration can be characterized by a singlet–triplet mixing angle  $\theta$ . The mixing angle can be independently determined from either the energies of the four  $nsnp$  levels, the decay rates of the two  $J = 1$  levels (to within factors of the radial transition element), or the magnetic  $g$ -factors of the levels with  $J > 0$ .

This mixing angle formulation has provided the basis for a semiempirical

**Table 1.** Measured lifetimes, compared with other experiments and theoretical values.

Level	$\lambda$ (Å)	$\tau$ (ns)		
		This work	Other expt	Theory
6s6p $^3P_1$	1908.7	39 ± 2		36 <sup>a</sup> , 74 <sup>b</sup> , 36 <sup>c</sup> , 40 <sup>d</sup> , 81 <sup>e</sup> , 44 <sup>f</sup>
6s6p $^1P_1$	1321.7	0.59 ± 0.04	0.65 ± 0.08 <sup>g</sup>	0.57 <sup>a</sup> , 0.58 <sup>b</sup> , 0.58 <sup>c</sup> , 0.57 <sup>d</sup> , 0.33 <sup>e</sup> , 0.34 <sup>f</sup>
6s6d $^1D_2$	2531	6.5 ± 0.5	5 ± 1 <sup>h</sup> , 7 ± 1 <sup>i</sup>	
6s7s $^1S_0$	3092	3.0 ± 0.4	4.6 ± 0.5 <sup>h</sup> , 3.9 ± 0.3 <sup>i</sup>	

<sup>a</sup> Brage *et al* [4], MCDF-AS<sub>5</sub>.

<sup>b</sup> Beck and Cai [5].

<sup>c</sup> Migdałek and Baylis [21].

<sup>d</sup> Migdałek and Bojara [22].

<sup>e</sup> Das and Idrees [23].

<sup>f</sup> Chou and Huang [24].

<sup>g</sup> Andersen *et al* [9].

<sup>h</sup> Andersen and Sørensen [10].

<sup>i</sup> Zhuvikin *et al* [11].

parametrization [25, 26] in which spectroscopic data are exploited to characterize the singlet–triplet mixing angle, which is then used to remove the effects of intermediate coupling from measured line strength data for both the resonance and intercombination transitions. This provides an empirical exposition of the squared dipole transition element that is well suited to isoelectronic interpolation and extrapolation. This formalism has been applied to the  $ns^2$ – $nsnp$  transitions in the Be ( $n = 2$ ) [8], Mg ( $n = 3$ ) [26], Zn ( $n = 4$ ) [27], Cd ( $n = 5$ ) [6] and Hg ( $n = 6$ ) [6] sequences. Moreover, it has been observed that the measured data tend to approach a value at very high  $Z$  which can be predicted by hydrogenic calculations [7, 8].

For the unbranched  $J = 0 - 1$  resonance and intercombination transitions, the line strengths  $S(\text{Res})$  and  $S(\text{Int})$  can be deduced from the lifetime  $\tau$  and the transition wavelength  $\lambda$  using

$$S = [\lambda(\text{Å})/1265.38]^3 3/\tau \text{ (ns)}. \quad (1)$$

In the absence of significant configuration interaction, the singlet–triplet mixing angle  $\theta$  can be deduced from the energies of the 6s6p  $^3P_0$ ,  $^3P_1$ ,  $^3P_2$  and  $^1P_1$  levels using

$$\cot(2\theta) = \frac{1}{\sqrt{2}}(\varepsilon_2 - 3\varepsilon_1 + 2\varepsilon_0)/(\varepsilon_2 - \varepsilon_0) \quad (2)$$

where  $\varepsilon_J$  is the energy or average energy of the level or levels with angular momentum  $J$ . These values for  $\theta$  can be used to further convert measured lifetime data to the reduced line strengths  $S_r(\text{Res})$  and  $S_r(\text{Int})$

$$S_r(\text{Res}) \equiv S(\text{Res})/\cos^2 \theta; \quad S_r(\text{Int}) \equiv S(\text{Int})/\sin^2 \theta \quad (3)$$

which are proportional to the squared radial transition matrices. It has been observed that line strengths can often be represented for interpolation and critical evaluation by an empirical relationship

$$Z^2 S_r \cong S_0 + B/(Z - C) \quad (4)$$

where  $Z$  is the nuclear charge,  $B$  and  $C$  are least-squares-adjusted fitting constants, and  $S_0$  is obtained either by least-squares fitting or as a theoretical asymptotic limit. Often the trends

extrapolate to values at infinite  $Z$  which correspond to the hydrogenic limit  $S_H$  (neglecting effects of the asymptotic degeneracy of levels in the same complex discussed in [8])

$$S_0 \cong S_H = 9n^2(n^2 - 1)/2. \quad (5)$$

Thus, one goal of this study was to investigate the degree to which the trends of theoretical and experimental data displayed in this exposition approach the  $n = 6$  value  $S_H = 5670$  in the high- $Z$  limit.

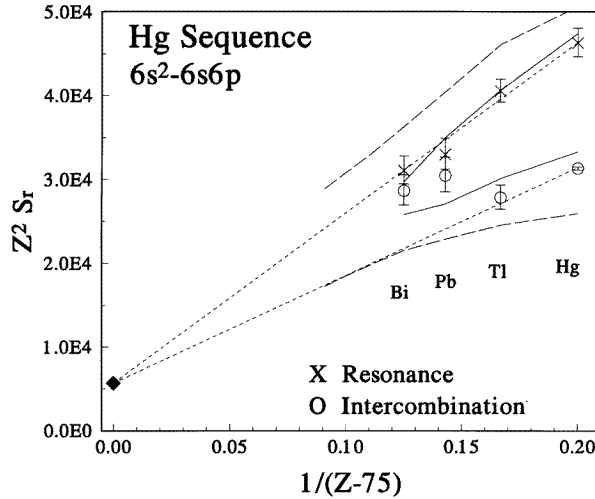


**Figure 1.** Plot of charge-scaled reduced line strength against reciprocal screened charge. Symbols denote measured values for the resonance ( $\times$ ) and intercombination ( $\circ$ ) transitions. Curves trace MCRHF-CP calculations with a standardized model-potential (— — —), and a semiempirical alternative (—) with cutoff radii adjusted to match measured ionization potentials. Lines (- - -) connect Hg I measurements with the high- $Z$  asymptote ( $\blacklozenge$ ).

**Table 2.** Isoelectronic comparisons of lifetimes and reduced oscillator strengths (with quoted and propagated uncertainties in parentheses).

$Z$	Ion	$\lambda_R$ (Å)	$\tau_R$ (ns)	$Z^2 S_r$ (Res)	$\lambda_I$ (Å)	$\tau_I$ (ns)	$Z^2 S_r$ (Int)	$\sin \theta$
80	Hg I	1849.5	1.34(3) <sup>a</sup>	$463(17) \times 10^2$	2573.3	118.9(4) <sup>b</sup>	$313(2) \times 10^2$	0.2030
81	Tl II	1321.7	0.59(4) <sup>c</sup>	$405(14) \times 10^2$	1908.8	39(3) <sup>c</sup>	$278(14) \times 10^2$	0.2495
82	Pb III	1048.9	0.381(21) <sup>d</sup>	$330(18) \times 10^2$	1553.0	14.8(10) <sup>d</sup>	$305(21) \times 10^2$	0.2876
83	Bi IV	872.6	0.243(13) <sup>e</sup>	$310(17) \times 10^2$	1317.1	8.0(5) <sup>f</sup>	$286(18) \times 10^2$	0.3189

<sup>a</sup> Weighted average of twelve measurements tabulated in [29]

<sup>b</sup> Weighted average of six measurements reported in [30–35].

<sup>c</sup> This work.

<sup>d</sup> Ansbacher *et al* [36].

<sup>e</sup> Ansbacher *et al* [37].

<sup>f</sup> Pinnington *et al* [38].

A summary of the existing lifetime data for the  $6s^2$ – $6s6p$  transitions in the Hg isoelectronic sequence is given in table 2, together with values obtained for the mixing angles and reduced line strengths. These data are presented in a plot of reduced line strengths against  $1/(Z - 75)$  in figure 1 (the value  $C = 75$  was chosen to yield reasonable

linearity as described in equation (4)). The long-dashed curves trace multiconfiguration relativistic Hartree–Fock calculations by Migdalek and Baylis [21] which used a model potential to represent core polarization (MCRHF-CP). The full curves indicate an alternative semiempirical version of this calculation [21] which adjusts the cut-off radius in the core polarization potential to match experimental ionization energies. Other isoelectronic calculations that do not include core polarization [24] have been demonstrated to differ significantly from established trends [28] and were omitted from the plot. The tendencies for both the measurements and the theoretical calculations approach the high- $Z$  hydrogenic limit is emphasized in figure 1 by short-dashed lines which connect Hg I data with the limiting value  $Z^2S \Rightarrow 5670$ .

We are grateful to Drs Donald Beck, Tomas Brage, David Ellis, Indrek Martinson, Eric Pinnington and Glenn Wahlgren for valuable discussions. The work was supported by the US Department of Energy, Office of Basic Energy Sciences, Division of Chemical Sciences, under Grant number DE-FG02-94ER14461.

## References

- [1] Leckrone D S, Johansson S G, Kalus G, Wahlgren G W and Brage T 1996 *Astrophys. J.* **462** 937
- [2] Johansson S G, Kalus G, Brage T, Leckrone D S and Wahlgren G W 1996 *Astrophys. J.* **462** 943
- [3] Dehmelt H G 1982 *IEEE Trans. Instrum. Meas.* **IM-31** 83
- [4] Brage T, Leckrone D S and Froese Fischer C 1996 *Phys. Rev. A* **53** 192
- [5] Beck D R and Cai Z 1990 *Phys. Rev. A* **41** 301
- [6] Curtis L J 1993 *J. Phys. B: At. Mol. Opt. Phys.* **26** L589
- [7] Curtis L J, Ellis D G and Martinson I 1995 *Phys. Rev. A* **51** 251
- [8] Curtis L J and Ellis D G 1996 *J. Phys. B: At. Mol. Opt. Phys.* **29** 645
- [9] Andersen T, Kirkegård Nielsen A and Sørensen G 1972 *Phys. Scr.* **6** 122
- [10] Andersen T and Sørensen G 1972 *Phys. Rev. A* **5** 2447
- [11] Zhuvikin G V, Penkin N P and Shabanova L N 1977 *Opt. Spektrosk.* **42** 236
- [12] Curtis L J, Berry H G and Bromander J 1971 *Phys. Lett.* **34A** 169
- [13] Curtis L J 1976 Lifetime Measurements *Beam Foil Spectroscopy* ed S Bashkin (Berlin: Springer) pp 63–109
- [14] Beideck D J, Curtis L J, Irving R E, Maniak S T, Hellborg R, Johansson S G, Joueizadeh A A and Martinson I 1993 *Phys. Rev. A* **47** 884
- [15] Henderson M, Bengtsson P, Corcoran J, Curtis L J, Irving R E and Maniak S T 1996 *Phys. Scr.* **53** 309
- [16] Haar R R, Beideck D J, Curtis L J, Kvale T J, Sen A, Schechtman R M and Stevens H W 1993 *Nucl. Instrum. Methods B* **79** 746
- [17] Haar R R and Curtis L J 1993 *Nucl. Instrum. Methods B* **79** 782
- [18] Provencher S W 1976 *J. Chem. Phys.* **64** 2772
- [19] Engström L 1982 *Nucl. Instrum. Methods* **202** 369
- [20] Sigmund P and Winterbon K B 1974 *Nucl. Instrum. Methods* **119** 541
- [21] Migdalek J and Baylis W E 1985 *J. Phys. B: At. Mol. Phys.* **18** 1533
- [22] Migdalek J and Bojara A 1988 *J. Phys. B: At. Mol. Opt. Phys.* **21** 2221
- [23] Das B P and Idrees M 1990 *Phys. Rev. A* **42** 6900
- [24] Chou H-S and Huang K-N 1992 *Phys. Rev. A* **45** 1403
- [25] Curtis L J 1989 *Phys. Rev. A* **40** 6958
- [26] Curtis L J 1991 *Phys. Scr.* **43** 137
- [27] Träbert E and Curtis L J 1993 *Phys. Scr.* **48** 586
- [28] Pinnington E H and Baylis W E 1992 *Phys. Rev. A* **46** 7325
- [29] Benck E C, Lawler J E and Dakin J T 1989 *J. Opt. Soc. Am. B* **6** 11
- [30] Andersen T and Sørensen G 1973 *J. Quant. Spectrosc. Radiat. Transfer* **13** 369
- [31] Lurio A 1965 *Phys. Rev.* **140** A 1505
- [32] Skerbele A and Lassette E N 1972 *J. Chem. Phys.* **52** 2708
- [33] Abjean R and Johannin-Gilles A 1976 *J. Quant. Spectrosc. Radiat. Transfer* **16** 369
- [34] Jean P, Martin M and Lecler D 1967 *C. R. Seances Acad. Sci. Ser. B* **264** 1791
- [35] Pinnington E H, Ansbacher W, Kernahan J A, Ahmad T and Ge Z-Q 1988 *Can. J. Phys.* **66** 960

- [36] Ansbacher W, Pinnington E H and Kernahan J A 1988 *Can. J. Phys.* **66** 402
- [37] Ansbacher W, Pinnington E H, Tauheed A and Kernahan J A 1989 *Phys. Scr.* **40** 454
- [38] Pinnington E H, Ansbacher W, Kernahan J A, Ge Z-Q and Inamdar A S 1988 *Nucl. Instrum. Methods B* **31**  
206